qualitative analysis.

Quantitative curve matching analysis, based on the residual map, should also be made to the typical anomalies on the residual map.

The method, which will be used in this analytical work, are summarized in the following section. The flow chart of analyses in shown in Fig. III–2.

2–7–1 Spectral Analysis

The wavelength characteristics of magnetic anomalies distributed over the survey area is effectively applied to make a magnetic analysis through filtering as well as to estimate the depth to the magnetic basement by using the potential theory.

1) Energy Spectrum

An observed value $F(x,y)$ in the rectangular coordinates is expressed in two-dimensional Fourier transform series as shown in equation (1).

$$F(x,y)=\int_0^{\infty}\int_0^{\infty} Amn\ exp(-2\pi j\ (\frac{mx}{L_1}+\frac{ny}{L_2}))\,dmdn \qquad (1)$$

Then, the Fourier coefficient Amn is given by

$$Amn=\frac{4}{L_1L_2}\int_0^{L1}\int_0^{L2} F(x,y)\ exp(2\pi j\ (\frac{mx}{L_1}+\frac{ny}{L_2}))\ dxdy \qquad (2)$$

where the value of F(x,y) is distributed uniformly over an area of L1 x L2 and $j=\sqrt{-1}$.

For a computer use, the data of F(x,y) are given or a rectangular grid with spacings of Δx and Δy, i.e. F(i,j) at the (i,j) the grid point by defining $x=i.\Delta x$ and $y=j.\Delta y$. Equation (2) can be written in the form:

$$Amn=\frac{4}{L_1L_2}\Delta x\Delta y\sum_{i=0}^{L2/\Delta x}\sum_{j=0}^{L2/\Delta x} Wij\cdot F(i,j)\,exp(2\pi j\,(\frac{m\cdot i\cdot \Delta x}{L_1}+\frac{n\cdot j\cdot \Delta y}{L_2})) \qquad (3)$$

where Wij is the weight in the two-dimensional trapezoidal rule of numerical integration.

The energy spectrum is obtained as

$$Emn=\left|Amn\right|^2 \qquad (4)$$

2) Estimation of Mean Depth to Magnetic Basement

Assuming that an energy spectrum of magnetic anomalies due to a magnetic layer lying at a depth of H is "white", the potential theory leads the following relation between energy spectrum Emn of wavenumber (m, n) and H. It is

$$Emn \propto exp(-4\pi Hf), \qquad (5)$$

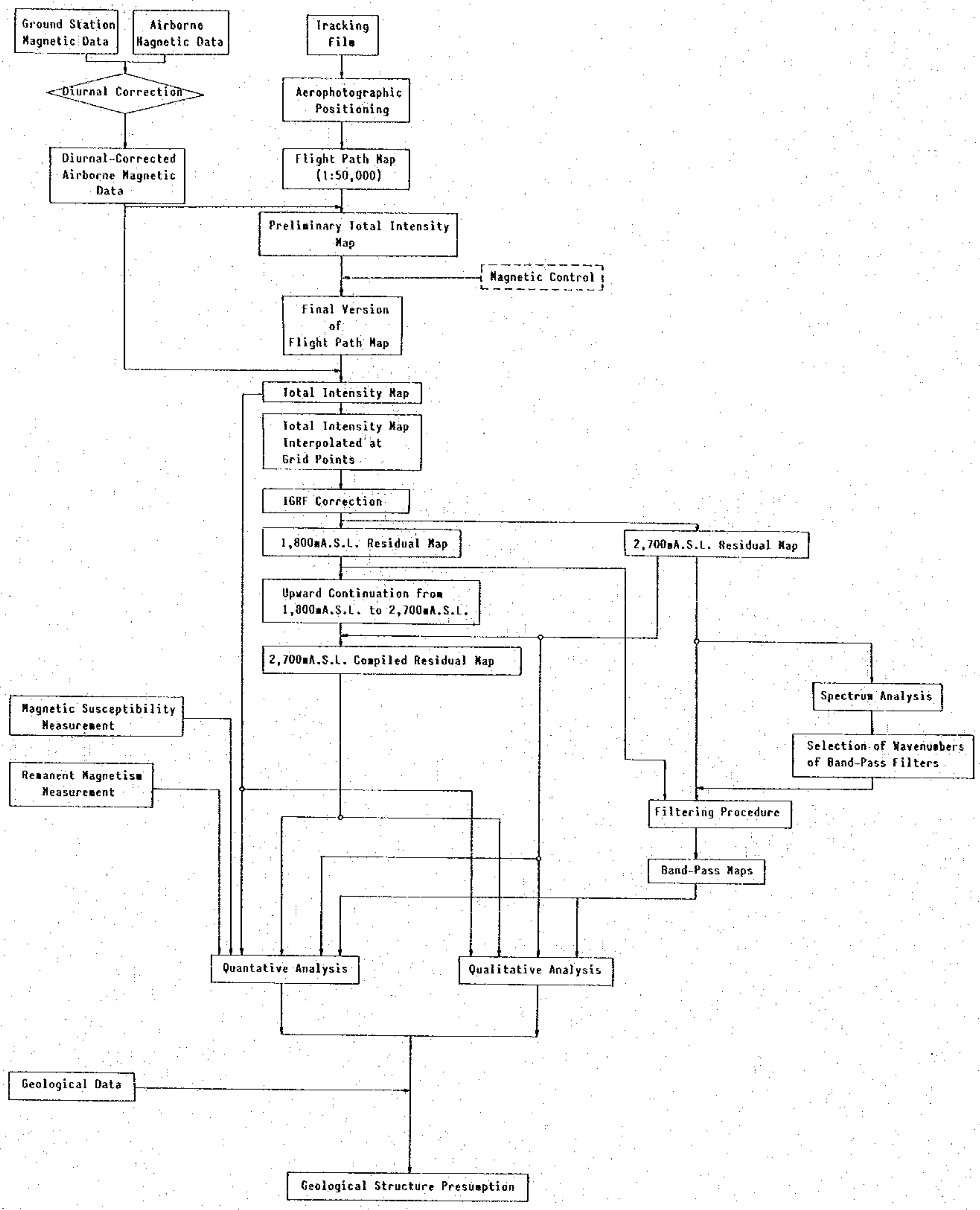

Fig. Ⅲ-2 Flow Chart of Data Processing and Analyses

Table Ⅲ-1 Coefficients of Upward Continuation Filter

(Continuation level = −1.8 x Data Interval)

Coefficients of Large Operator

	m= 0	m= 1	m= 2	m= 3	m= 4	m= 5	m= 6	m= 7	m= 8	m= 9	m=10	m=11	m=12	m=13	m=14	m=15
n= 0	+0.04840	+0.03296	+0.01455	+0.00678	+0.00334	+0.00195	+0.00114	+0.00078	+0.00050	+0.00038	+0.00026	+0.00021	+0.00015	+0.00013	+0.00010	+0.00009
n= 1	+0.03296	+0.01408	+0.01206	+0.00598	+0.00312	+0.00183	+0.00111	+0.00075	+0.00050	+0.00037	+0.00026	+0.00021	+0.00016	+0.00013	+0.00010	+0.00008
n= 2	+0.01455	+0.01206	+0.00759	+0.00438	+0.00256	+0.00157	+0.00101	+0.00063	+0.00048	+0.00035	+0.00026	+0.00020	+0.00015	+0.00012	+0.00010	+0.00008
n= 3	+0.00678	+0.00598	+0.00438	+0.00293	+0.00191	+0.00126	+0.00085	+0.00060	+0.00043	+0.00032	+0.00024	+0.00019	+0.00015	+0.00012	+0.00010	+0.00008
n= 4	+0.00334	+0.00312	+0.00256	+0.00191	+0.00137	+0.00097	+0.00070	+0.00051	+0.00038	+0.00029	+0.00022	+0.00017	+0.00014	+0.00011	+0.00009	+0.00007
n= 5	+0.00195	+0.00183	+0.00157	+0.00126	+0.00097	+0.00074	+0.00056	+0.00042	+0.00032	+0.00025	+0.00020	+0.00016	+0.00013	+0.00010	+0.00009	+0.00007
n= 6	+0.00114	+0.00111	+0.00101	+0.00085	+0.00070	+0.00056	+0.00044	+0.00035	+0.00027	+0.00022	+0.00017	+0.00014	+0.00012	+0.00010	+0.00008	+0.00007
n= 7	+0.00078	+0.00075	+0.00068	+0.00060	+0.00051	+0.00042	+0.00035	+0.00028	+0.00023	+0.00019	+0.00015	+0.00013	+0.00010	+0.00009	+0.00007	+0.00006
n= 8	+0.00050	+0.00050	+0.00048	+0.00043	+0.00038	+0.00032	+0.00027	+0.00023	+0.00019	+0.00016	+0.00013	+0.00011	+0.00009	+0.00008	+0.00007	+0.00006
n= 9	+0.00038	+0.00037	+0.00035	+0.00032	+0.00029	+0.00025	+0.00022	+0.00019	+0.00016	+0.00013	+0.00011	+0.00010	+0.00008	+0.00007	+0.00006	+0.00005
n=10	+0.00026	+0.00026	+0.00026	+0.00024	+0.00022	+0.00020	+0.00017	+0.00015	+0.00013	+0.00011	+0.00010	+0.00009	+0.00007	+0.00006	+0.00006	+0.00005
n=11	+0.00021	+0.00021	+0.00020	+0.00019	+0.00017	+0.00016	+0.00014	+0.00013	+0.00011	+0.00010	+0.00009	+0.00007	+0.00007	+0.00006	+0.00005	+0.00004
n=12	+0.00015	+0.00016	+0.00015	+0.00015	+0.00014	+0.00013	+0.00012	+0.00010	+0.00009	+0.00008	+0.00007	+0.00007	+0.00006	+0.00005	+0.00004	+0.00004
n=13	+0.00013	+0.00013	+0.00012	+0.00012	+0.00011	+0.00010	+0.00010	+0.00009	+0.00008	+0.00007	+0.00006	+0.00006	+0.00005	+0.00005	+0.00004	+0.00004
n=14	+0.00010	+0.00010	+0.00010	+0.00010	+0.00009	+0.00009	+0.00008	+0.00007	+0.00007	+0.00006	+0.00006	+0.00005	+0.00004	+0.00004	+0.00004	+0.00003
n=15	+0.00009	+0.00008	+0.00008	+0.00008	+0.00007	+0.00007	+0.00007	+0.00006	+0.00006	+0.00005	+0.00005	+0.00004	+0.00004	+0.00004	+0.00003	+0.00003

Small Operator for Upward Continuation

	m= 0	m= 1	m= 2	m= 3	m= 4	m= 5
n= 0	+0.06034	+0.04110	+0.01814	+0.00845	+0.00417	+0.00143
n= 1	+0.04110	+0.03002	+0.01503	+0.00746	+0.00389	+0.00228
n= 2	+0.01814	+0.01503	+0.00947	+0.00546	+0.00319	+0.00195
n= 3	+0.00845	+0.00746	+0.00546	+0.00365	+0.00238	+0.00157
n= 4	+0.00417	+0.00389	+0.00319	+0.00238	+0.00171	+0.00121
n= 5	+0.00243	+0.00228	+0.00195	+0.00157	+0.00121	+0.00092

where f is a quantity called frequency :

$$f = \sqrt{(\frac{m}{L_1})^2 + (\frac{n}{L_2})^2} \qquad (6)$$

The energy spectrum is plotted in an f vz. log Emn graph. A straight line is determined by the least square fitting to the plots. Taking equation (5) into consideration, H is derived from the tangent of the straight line.

2–7–2 Band-Pass Filter

The band-pass filter is derived from the deviation between two low-pass filter whose cut-off frequencies are different from each other. Band pass operators designed by P.M. Lavin et al (1970) were adapted and the outline is given as follows:

The impulse response of an ideal two-dimensional wavenumber filter with circular symmetry is a function of the radius variable $r(r^2 = x^2+y^2)$, i.e.,

$$w(x, y) = w(r) \qquad (7)$$

And the wavenumber response of equation (7) is also a circularly symmetric function of the wavenumber variable k,

$$W(kx, ky) = W(k), \qquad (8)$$

where kx and ky are wavenumbers in the x and y directions respectively, and $k^2=kx^2+ky^2$. The impulse and wavenumber responses are related by the Hankel transform pair

$$W(k) = \pi \int_0^\infty w(r) Jo(2\pi kr) dr \qquad (9)$$

and

$$w(r) = 2\pi \int_0^\infty W(k) Jo(2\pi kr) kdk \qquad (10)$$

The response of an ideal low-pass filter is given by

$$W(k) = 1, \quad |k| \leqq k_c$$
$$= 0, \quad |k| > k_c \qquad (11)$$

where kc is the desired cut-off wavenumber. The impulse response (inverse transform) is

$$w(r) = \pi \int_0^{kc} Jo(2\pi kr) kdk = \frac{k_c J_1(2\pi k_c r)}{\gamma} \qquad (12)$$

It is desirable to specify a wavenumber response that has a smooth cut-off region, i.e., and absence of a discontinuity at the cut-off wavenumber.

The transfer function of the desired filter is expressed by

$$W(k) = \int_0^{\infty}\int_0^{2\pi} H(k')\,G(K)\,k'\,dk'\,dp, \tag{13}$$

where $K^2 = k^2 + (k')^2 - 2\,kk'\cos\phi$ (14)

Since convolution in the wavenumber domain is equivalent to multiplication in the space domain, the weighting function (impulse response) is given by

Let $w(r) = h(r)\,g(r)$. (15)

$$\begin{aligned} G(k) &= 1\,, \quad |k| \leqq a, \\ &= 0\,, \quad |k| > a, \end{aligned} \tag{16}$$

where a=(kc+kt)/2, kc is the desired cut-off wavenumber, and kt is the desired termination wavemember of the filter. The inverse transform of equation (16) is

$$g(r) = \frac{aJ_1(2\pi ar)}{r} \tag{17}$$

And, let

$$\begin{aligned} H(k) &= \beta \cdot Jo(\alpha k/\Delta k), \quad |k| \leqq \Delta k/2 \\ &= 0 \qquad\qquad\qquad , \quad |k| > \Delta k/2 \end{aligned} \tag{18}$$

where Δk = kt−kc and α and β are constants,

Then,

$$\begin{aligned} H(k) &= \frac{\alpha}{\pi \Delta k^2 J_1(\alpha/2)} Jo\left(\frac{\alpha k}{\Delta k}\right), \quad |k| \leqq \frac{\Delta k}{2} \\ &= 0 \qquad\qquad\qquad\qquad\qquad , \quad |k| > \frac{\Delta k}{2} \end{aligned} \tag{19}$$

The inverse Hankel transform of equation (19) is

$$h(r) = 2\pi \int_0^{\Delta k/2} \frac{\alpha}{\pi \Delta k^2 J_1(\alpha/2)} Jo\left(\frac{\alpha k}{\Delta k}\right) Jo(2\pi rk)\,k\,dk = \frac{Jo(\pi r \Delta k)}{1-(2\pi r \Delta k/\alpha)^2} \tag{20}$$

Substituting equations (17) and (20) in equation (15), the desired impulse response is obtained as follows :

Table Ⅲ-2 Coefficients of Band-pass Filter

Coefficients of Large Operator

	M= 0	M= 1	M= 2	M= 3	M= 4	M= 5	M= 6	M= 7
n= 0	+5.870E-02	−3.162E-03	−4.524E-04	−7.304E-05	−3.015E-06	+1.851E-06	−1.147E-06	−9.625E-07
n= 1	−3.162E-03	−1.296E-03	−3.009E-04	−5.166E-05	−8.306E-07	+1.529E-06	−1.262E-06	−8.568E-07
n= 2	−4.524E-04	−3.009E-04	−1.029E-04	−1.655E-05	+2.148E-06	+5.055E-07	−1.443E-06	−5.190E-07
n= 3	−7.304E-05	−5.166E-05	−1.655E-05	+6.478E-07	+1.851E-06	−8.258E-07	−1.311E-06	+4.609E-08
n= 4	−3.015E-06	−8.306E-07	+2.148E-06	+1.851E-06	−3.791E-07	−1.454E-06	−6.338E-07	+6.896E-07
n= 5	+1.851E-06	+1.529E-06	+5.055E-07	−8.258E-07	−1.454E-06	−8.568E-07	+3.507E-07	+1.126E-06
n= 6	−1.147E-06	−1.262+-06	−1.443E-06	−1.311E-06	−6.338E-07	+3.507E-07	+1.068E-06	+1.132E-06
n= 7	−9.625E-07	−8.568E-07	−5.190E-07	+4.609E-08	+6.896E-07	+1.126E-06	+1.132E-06	+7.524E-07
n= 8	+6.129E-07	+6.896E-07	+8.858E-07	+1.100E-06	+1.187E-06	+1.040E-06	+6.834E-07	+2.840E-07
n= 9	+1.182E-06	+1.174E-06	+1.132E-06	+1.012E-06	+7.869E-07	+4.836E-07	+1.926E-07	+1.722E-08
n=10	+6.834E-07	+6.491E-07	+5.481E-07	+3.924E-07	+2.138E-07	+6.357E-08	−9.245E-09	+6.683E-09
n=11	+1.192E-07	+1.037E-07	+6.357E-08	+1.722E-08	−1.105E-08	−2.914E-09	+3.932E-08	+8.717E-08
n=12	−7.820E-09	−5.540E-09	+3.231E-09	+2.227E-08	+5.207E-08	+8.443E-08	+1.020E-07	+8.637E-08
n=13	+8.443E-08	+8.717E-08	+9.40 E-08	+1.009E-07	+1.004E-07	+8.373E-08	+4.523E-08	−1.131E-08
n=14	+7.795E-08	+7.482E-08	+6.459E-08	+4.523E-08	+1.518E-08	−2.424E-08	−6.656E-08	−1.002E-07

	M= 8	M= 9	M=10	M=11	M=12	M=13	M=14
n= 0	+6.129E-07	+1.182E-06	+6.834E-07	+1.192E-07	−7.820E-09	+8.443E-08	+7.795E-08
n= 1	+6.896E-07	+1.174E-06	+6.491E-07	+1.037E-07	−5.540E-09	+8.717E-08	+7.482E-08
n= 2	+8.858E-07	+1.132E-06	+5.481E-07	+6.357E-08	+3.231E-09	+9.407E-08	+6.459E-08
n= 3	+1.100E-06	+1.012E-06	+3.924E-07	+1.722E-08	+2.227E-08	+1.009E-07	+4.523E-08
n= 4	+1.187E-06	+7.869E-07	+2.138E-07	−1.105E-08	+5.207E-08	+1.004E-07	+1.518E-08
n= 5	+1.040E-06	+4.836E-07	+6.357E-08	−2.914E-09	+8.443E-08	+8.375E-08	−2.424E-08
n= 6	+6.834E-07	+1.926E-07	−9,245E-09	+3.932E-08	+3.932E-07	+4.523E-08	−6.656E-08
n= 7	+2.840E-07	+1.722E-08	+6.683E-09	+8.717E-08	+8.717E-08	−1.131E-08	−1.002E-07
n= 8	+3.285E-08	−5.540E-09	+6.793E-08	+1.004E-07	+3.264E-08	−6.985E-08	−1.126E-07
n= 9	−5.540E-09	+6.022E-08	+1.022E-07	+5.715E-08	−4.074E-08	−1.074E-07	−9.756E-08
n=10	+6.793E-08	+1.022E-07	+6.459E-08	−2.424E-08	−9.835E-08	−1.077E-07	−6.145E-08
n=11	+1.004E-07	+5.715E-08	−2.424E-08	−9.429E-08	−1.109E-07	−7.377E-08	−2.200E-08
n=12	+3.264E-08	−4.074E-08	−9.835E-08	−1.109E-07	−7.778E-08	−2.852E-08	+1.711E-09
n=13	−6.985E-08	−1.074E-07	−1.077E-07	−7.377E-08	−2.852E-08	+6.269E-10	+2.389E-09
n=14	−1.126E-07	−9.756E-08	−6.145E-08	−2.200E-08	+1.711E-09	+2.389E-09	−1.015E-08

* (−9.756E−08) means (-9.756×10^{-8}).

Coefficients of Small Operator

	M= 0	M= 1	M= 2	M= 3	M= 4	M= 5
n= 0	+5.885E-02	−3.171E-03	−4.536E-04	−7.324E-05	−3.023E-06	+1.856E-06
n= 1	−3.171E-03	−1.300E-03	−3.017E-04	−5.179E-05	−8.327E-07	+1.533E-06
n= 2	−4.536E-04	−3.017E-04	−1.031E-04	−1.659E-05	+2.154E-06	+5.068E-07
n= 3	−7.324E-05	−5.179E-05	−1.659E-05	+6.495E-07	+1.856E-06	−8.279E-07
n= 4	−3.023E-06	−8.327E-07	+2.154E-06	+1.856E-06	−3.801E-07	−1.458E-06
n= 5	+1.856E-06	+1.533E-06	+5.068E-07	−8.279E-07	−1.458E-06	−8.591E-07

$$w(0) = \pi a^2$$

$$w(\alpha/2\pi \Delta k) = \frac{\pi a \Delta k}{2} J_1\left(\frac{\alpha a}{\Delta k}\right) J_1\left(\frac{\alpha}{2}\right)$$

$$w(r) = \frac{a J_1(2\pi a r)}{r} \cdot \frac{J_0(\pi r \Delta k)}{1-(2\pi r \Delta k/\alpha)^2} \tag{21}$$

where

$$\alpha = 4.8096$$
$$a = (k_c + k_t)/2$$
$$\Delta k = k_t - k_c$$

For a computer use, the same procedure as upward-continuation is carried out.

2–7–3 Second Vertical Derivative Map

Second vertical method as one of the qualitative analyses is applied to emphasize short wavelength magnetic anomalies of the residual map and attenuate long wavelength anomalies.

The operator derived by Rosenbach, O. (1953) was adapted as the second vertical derivative filter, which are given in the following equation:

$$\frac{\partial^2 T}{\partial Z^2} = \frac{1}{S^2} \cdot \frac{1}{24}(96\Delta T_0 - 72\Delta T_1 - 32\Delta T_2 + 8\Delta T_4) \tag{22}$$

where S is a grid spacing,

$$\Delta T_1 = \frac{1}{4}\sum_{i=1}^{4} \Delta_{1i},\ \Delta T_2 = \frac{1}{4}\sum_{i=1}^{4} \Delta T_{2i}\ and\ \Delta T_4 = \frac{1}{8}\sum_{i=1}^{8} \Delta T_{4i} \tag{23}$$

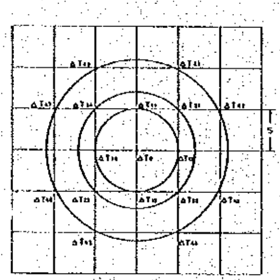

Fig. III–3 Point Configuration of Second Vertical Derivative Operator

2–8 Magnetic Properties of Rock Samples

A total of 54 rock samples were collected from outcrops at the location as shown in PL. 12. The sampling locations are distributed mainly in the western area of Mindoro Island. For all rock samples, the remanent magnetisms and magnetic susceptibilities are measured by means of spinner magnetometer and Bison 101 Susceptibility Meter, respectively. The results are shown in Table III–3.

The mean value of magnetic susceptibility amounts to :

916 x 10^{-6} emu/cc for basalt (Lumintao Formation of Baco Group, 10 samples),
820 x 10^{-6} emu/cc for ultramafic rock (4 samples),
20 x 10^{-6} emu/cc for Halcon Metamorphics (1 sample),
15 x 10^{-6} emu/cc for quartz diorite (2 samples),
12 x 10^{-6} emu/cc for sandstone (Mansalay Formation of Baco Group, 22 samples) and
12 x 10^{-6} emu/cc for limestone (Sablayan Group, 12 samples).

As mentioned above, the sampling locations are distributed especially in the central to northern part of the western area of Mindoro Island, so that it is difficult to classify the magnetic rocks in the whole area only from these data.

The results of the trial classification are as follows:

Strongly magnetic rocks: basalt and ultramafic rock

Slightly magnetic rocks ; Halcon Metamorphics, quartz diorite, sandstone and limestone.

From the above-mentioned results, it is observed that magnetic anomalies with short wavelength and large amplitude are dominant in the areas where strongly magnetic rocks are distributed, and the many magnetic anomlies of small amplitude corresponds to areas where slightly magnetic rocks are distributed.

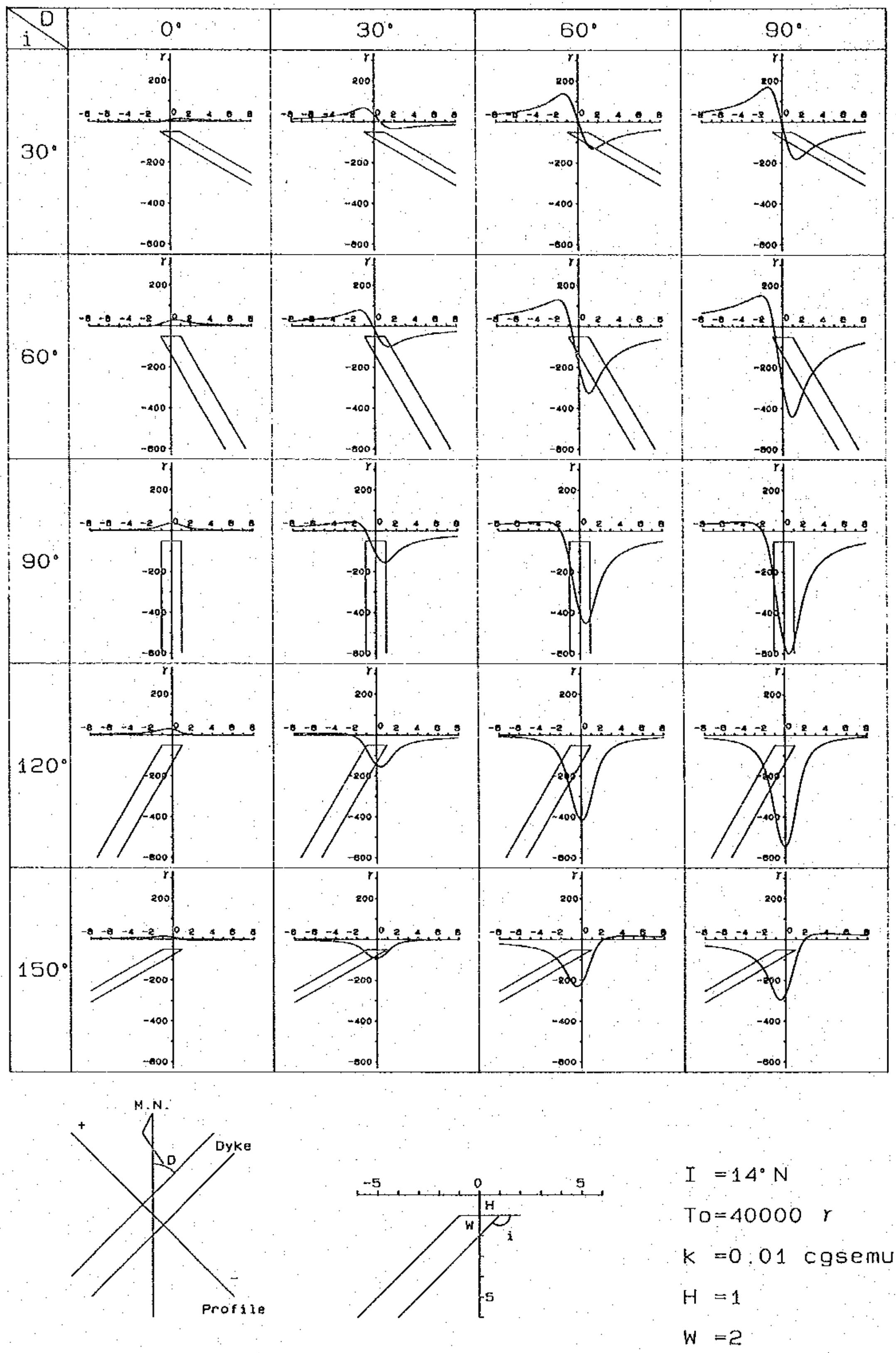

Fig. Ⅲ-4 Magnetic Anomaly due to Dike Model

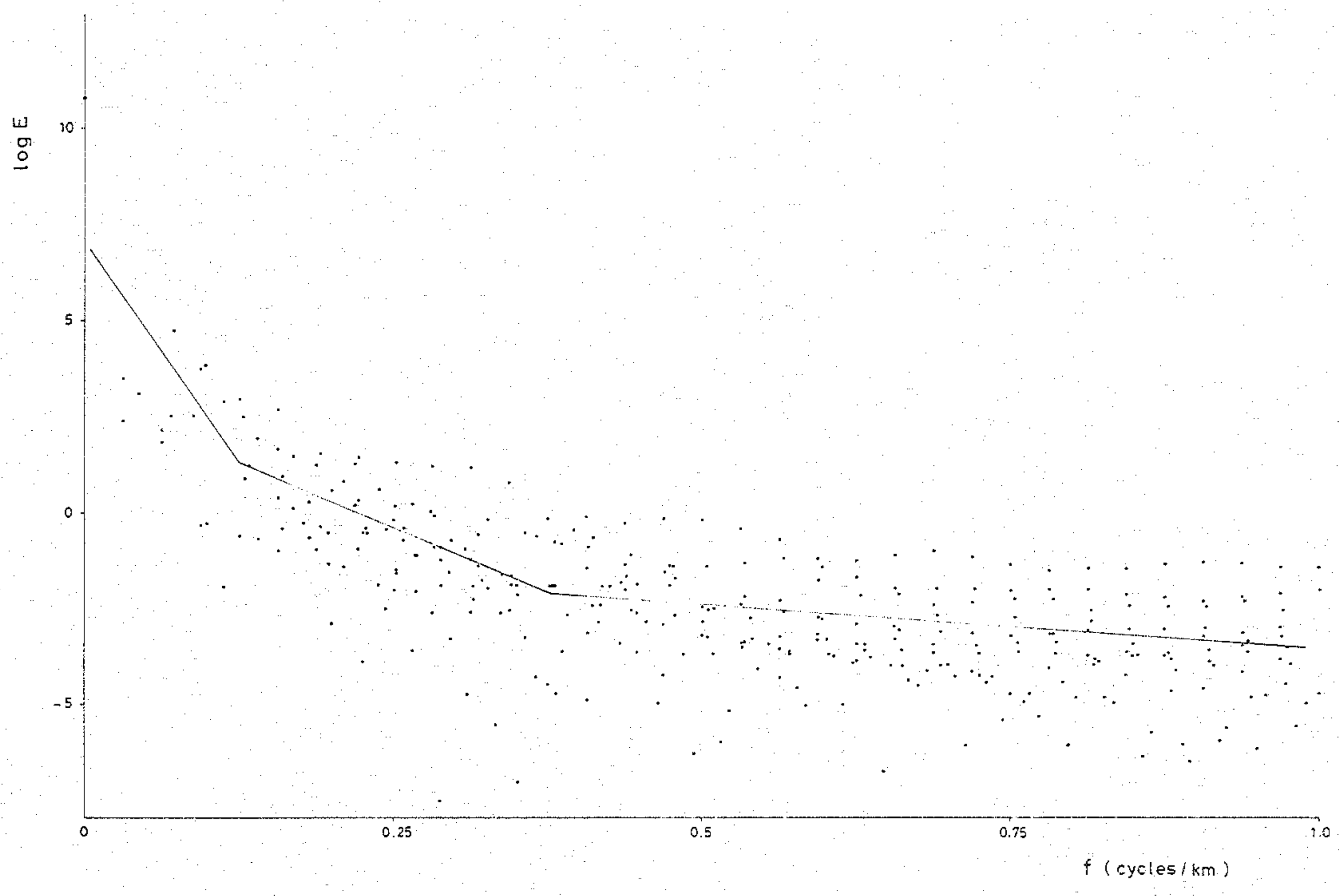

Fig. Ⅲ-5 Energy Spectrum vs. Wavenumber

Table Ⅲ-3 Magnetic Properties of Rock Samples

Group Name	Formation Name	Rock name	Sampling No.	Remanent Magnetism: Intensity ($\times 10^{-6}$ emu/cc)	Remanent Magnetism: Inclination	Remanent Magnetism: Declination	Susceptibility ($\times 10^{-6}$ emu/cc)	Average Susceptibility ($\times 10^{-6}$ emu/cc)
Sablayan Group		Limestone	A–3a	0.1	–57.3	S68.8W	1	
		Limestone	A–4a	0.3	–68.9	S60.0W	1	
		Limestone	A–7a	0.2	–10.9	N 9.3E	8	
		Limestone	A–11b	0.2	8.8	S69.9E	1	
		Limestone	A–13c	249.8	89.9	S 6.6E	7	
		Limestone	A–20a	0.3	44.5	N86.2W	8	12
		Limestone	A–62c	0.6	–7.1	S28.2E	4	
		Sandstone	A–29f	19.7	31.9	N85.8E	94	(12)*
		Sandstone	A–53f	0.3	–30.5	S70.4E	1	
		Conglomerate	A–54f	0.9	11.7	S19.7W	20	
		Siltstone	A–55b	0.8	–50.6	S43.2W	1	
		Siltstone	A–60c	1.4	–20.0	S48.3E	1	
Baco Group	Lumntao Formation	Basalt	A–8d	2,481.0	–75.7	N19.2E	104	
		Basalt	A–10b	237.6	8.8	N31.1W	599	
		Basalt	A–12b	260.1	41.9	S42.5E	778	
		Basalt	A–28c	1,249.0	70.4	N 8.5E	1,904	
		Metavolcanics	A–30b	7.2	26.5	S41.9W	(43)	
		Basalt	A–34b	364.7	–10.1	S85.3E	557	916
		Basalt	A–56b	3,420.0	–21.2	S47.2W	1,064	(10)*
		Basalt	A–57a	161.2	–6.3	S48.2W	653	
		Basalt	A–58a	2,192.0	–66.3	S48.8W	2,068	
		Basalt	A–59a	357.8	60.2	N60.9W	951	
		Basalt	A–69d	838.3	–2.8	S13.9E	481	
		Basalt	A–79a	2.9	79.0	N24.9E	(23)	
	Mansalay Formation	Sandstone	A–16a	4.9	63.6	N14.5W	14	
		Sandstone	A–17d	0.3	59.9	S45.5W	1	
		Sandstone	A–18b	2.0	–24.6	S39.9E	5	
		Sandstone	A–19b	2.3	84.6	N46.8W	10	
		Sandstone	A–23d	1.6	–44.1	S40.9E	13	
		Sandstone	A–24b	8.9	–12.6	S70.0E	25	
		Sandstone	A–25a	0.4	23.0	S11.1W	25	
		Sandstone	A–26c	1.9	–15.2	S72.3W	13	
		Sandstone	A–27b	2.8	–2.3	S 7.8E	18	12
		Sandstone	A–38f	2.4	32.6	S24.4W	10	
		Sandstone	A–42a	1.9	–5.2	S56.0E	32	(22)*
		Sandstone	A–66f	0.2	–44.7	N32.2E	13	
		Sandstone	A–67a–3	0.1	–6.3	S29.0W	6	
		Sandstone	A–68d	0.2	–60.8	S 0.9W	1	
		Sandstone	A–71a–2	0.6	16.0	S 5.2W	5	
		Sandstone	A–72b	0.5	–12.3	S47.5W	4	
		Fine sandstone	A–74c	0.3	–22.2	S27.5E	8	
		Fine sandstone	A–77a	1.3	77.0	S69.2E	10	
		Limestone	A–21a	0.2	–25.7	S 9.4W	8	
		Mudstone	A–22d	0.5	–28.1	S84.4W	14	
		Slate	A–73d	0.3	–20.5	N56.3W	19	
		Slate	A–78b	0.5	–5.0	S76.7E	17	
Halcon Metamorphics		Slate	A–43c	0.5	63.8	S24.8E	20	20(1)*
Quartz diorite		Quartz diorite	A–75c	4.6	–12.0	S 7.2E	13	15(2)*
		Quartz diorite	A–76c	1.2	–39.1	S48.8W	17	
Ultramafic Rock		Serpentinized dunite	A–33c	546.0	36.6	S27.8E	217	
		Serpentinized pyroxenite	A–39b	435.5	–5.0	S21.5E	814	
		Serpentinite	A–47d	513.8	–29.8	S66.0W	1,872	820(4)*
		Gabbro	A–49e	28.3	–74.0	S85.1W	(13)	
		Pyroxenite	A–70d	1,176.0	44.4	S39.6E	374	

* Number of rock samples used for calculation of average

3. Results of Analysis and Summary

Although interpretation should be made qualitatively and quantitatively on the basis of the residual map and its filtered maps, in this report, only the qualitative analysis of the total magnetic intensity map was made because of the delay of the completion of the residual maps. The result of qualitative analysis are described in the following section.

3–1 Results of Analysis

According to the total magnetic intensity map, the survey area (Mindoro Island) is classified into three areas:

Area I (southern area of Mindoro Island) : Iso-gamma lines with E–W trends are dominant and there are no characteristics of relief which suggests that magnetized bodies do not exist in the area. It also infers that sedimentary rocks are broadly distributed.

Area II (central area) : Iso-gamma lines of NW–SE trends are dominant and magnetic anomalies with half wavelength of 5 to 10 km are distributed in the NW direction. These represent the short wavelength, high amplitude anomalies which signifies the wide distribution of ultramafic rocks in the same direction.

Area III (northern area) : At the extreme northern portion of the survey area, high magnetic anomaly of large amplitude and long wavelength trending E–W is detected. Still it would be difficult to assume the shape of magnetic bodies causing this high anomaly because of the absence of the low magnetic anomaly which should appear in the offshore area not covered by the survey. At the southern side of this high anomaly, several small magnetic anomalies trending ENE–WSE ~ NE–SW distorts the iso-gamma lines. These distortions may be caused by small-size magnetic bodies.

Magnetic discontinuity lines (geotectonic lineaments) are judged from the magnetic features as like the distortions of iso-gamma lines and the continuity of magnetic anomalies. This magnetic discontinuity line seems to reflect the differences of the magnetic properties of the rocks consisting the earth. These lines do not always coincide with geotectonic lines in a geological sense but it may be understood that they may correspond to lithologic contact and/or faults.

The distribution of the geotectonic lineaments are as follows:

Area I : No existence of geotectonic lineaments are assumed.

Area II : Judging from the continuities of magnetic anomalies, geotectonic lineaments of NW–SE and NNW–SSE trends are assumed. Large geotectonic lineaments are listed as follows :

- II–A : Geotectonic lineament running from Mt. Pamucuban to Mt. Fetchel.
- II–B : Geotectonic lineament extending in a SSE direction from the west of Calapan at the north-central part of Mindoro, running parallel along Rosanna River in the central part to the vicinity of Roxas in the southeast coast of Mindoro.
- III–C : Geotectonic lineament running in a WNW–ESE direction from the east of Lake Naujan to Bongabong in the east coast.

Area III : It is assumed that geotectonic lineaments in ENE–WSW and NE–SW directions are dominant in the northwestern area based on the distortions of iso-gamma lines.

Judging from the difference between the directions of trends of dominant geotectonic lineaments of area II and III, it may be safe to assume that the geological structures between both areas are different from each other.

At present, only the magnetic susceptibility of the rock samples obtained mostly in the western part of Mindoro is available. Therefore, because of insufficient data, it would be difficult to assume the rock types causing the magnetic anomalies in some areas. The relationship between magnetic anomalies and the lithology can not yet be established. The results of qualitative interpretation of the typical anomalies after correlating with the geologic map are as follows:

Major magnetic anomalies observed on the total intensity map coincide with the distribution of the ultramafic rocks.

Area II : Magnetic anomalies are distributed at the north side of above-mentioned geotectonic lineaments, i.e., II–A, II–B and II–C, which may be caused by the ultramafic rocks.

In the area from Mt. Masombrero in the northern west coast through Santa Cruz and Mt. baco, magnetic anomalies that are distributed parallel with the geotectonic lineaments in NW–SE direction, may be caused also by the ultramafic rocks. Among these magnetic anomalies, a large scale magnetic anomaly is detected south of Mt. Baco, where the Lumintao Formation of the Baco Group is widely distributed on the geological map. This anomaly may be caused by either the exposed basaltic rocks of the Lumintao Formation or the ultramafic rocks concealed, from its large relief.

On the other hand, in the vicinity of Lake Naujan at the northeastern part of Area II, several small scale magnetic anomalies which may be caused by Quaternary volcanics are detected. A magnetic anomaly near Mt. Dumale may be caused by volcanic rocks. It may be possible that a highly magnetized body of large scale may be distributed at depth in the area north of Lake Naujan to the northern offshore area.

Area III : Highly magnetized bodies of large scale may exist at depth in the area from the north coast towards the sea. It is difficult to estimate magnetized bodies at the south side of this very high magnetic anomaly, but highly magnetic bodies may possibly exist along the aforementioned geotectonic lineaments trending NE and ENE. Correlating with the geological map, these anomalies may correspond to the ultramafic rocks.

3–2 Summary

Summary of the results of interpretation are as follows:

(1) Southern Mindoro (Area I) is consisted mainly of sedimentary rocks which do not show any magnetic property.

(2) In central Mindoro (Area II), ultramafic rocks are dominantly distributed along the geotectonic lineaments trending NW and NNW. A large-scale, highly magnetized body is assumed to appear at the south side of Mt. Baco, but from the geological information available, it is still doubtful to assume the rock types causing the anomaly. It is therefore recommended to conduct ground truth geological checking of that locality.

(3) Geotectonic lineaments trending NE and ENE dominates the northwestern area of Mindoro (Area III). From the difference in trends of lineaments in Area II and Area III it is assumed that their geologic structures are different from one another.

The interpretation results are shown on Plates III–11–1, III–11–2 and III–12. The structural profile is shown on Fig. III–6.

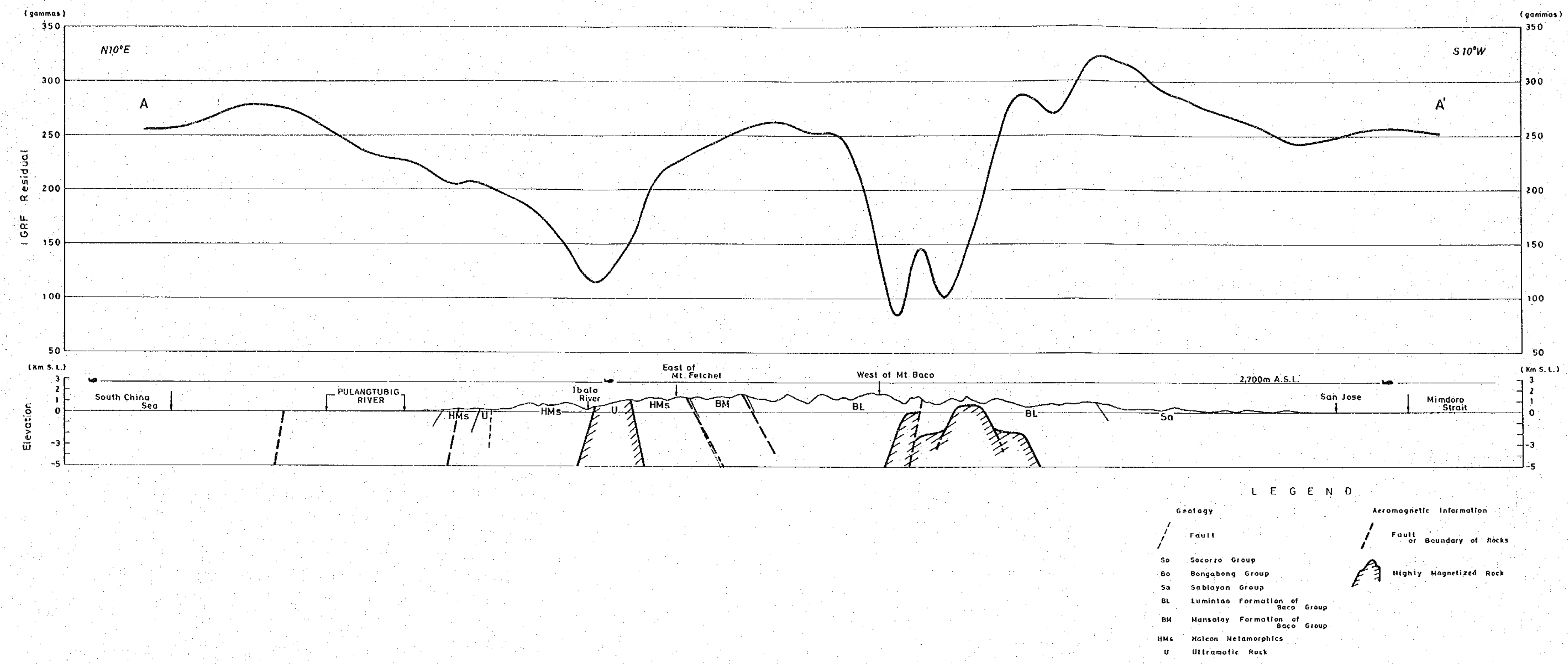

Fig. III-6 Structural Profile

APPENDICES

Fig. A-1 Microphotograph of Thin Section

Abbreviation

q	:	quartz
pl	:	plagioclase
bt	:	biotite
mus	:	muscovite
hb	:	hornblende
au	:	augite
hy	:	hypersthene
ol	:	olivine
en	:	enstatite
act	:	actinolite
ga	:	garnet
op	:	opaque minerals
ep	:	epidote
ser	:	sericite
chl	:	chlorite
srp	:	serpentine

Only lower polar

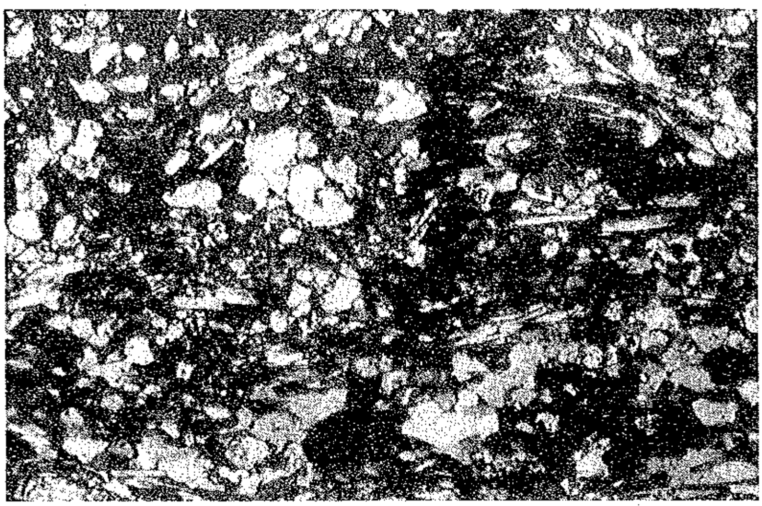

Crossed polars

0 0.5mm

Sample No. : SR–18
Location : Mananao River
Rock name : epidote actinolite schist
Group name : Halcon metamorphics

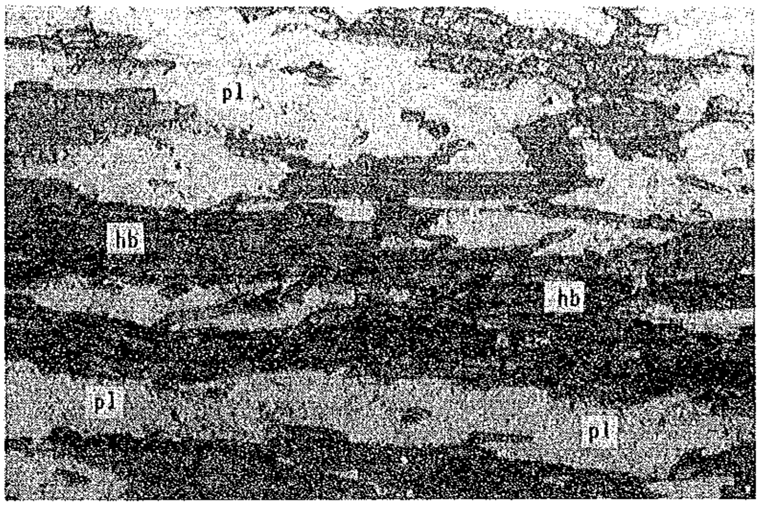

Only lower polar

Crossed polars

0 0.5mm

Sample No.	:	WR–12
Location	:	Bongabong River
Rock name	:	amphibolite
Group name	:	Halcon metamorphics

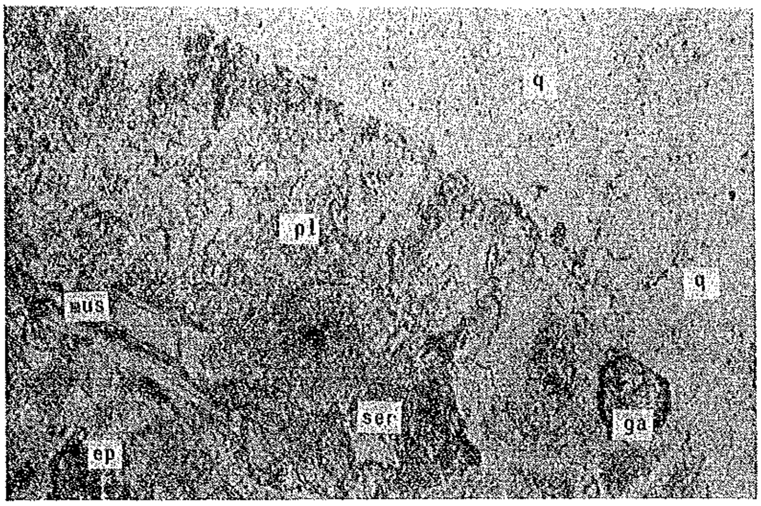

Only lower polar

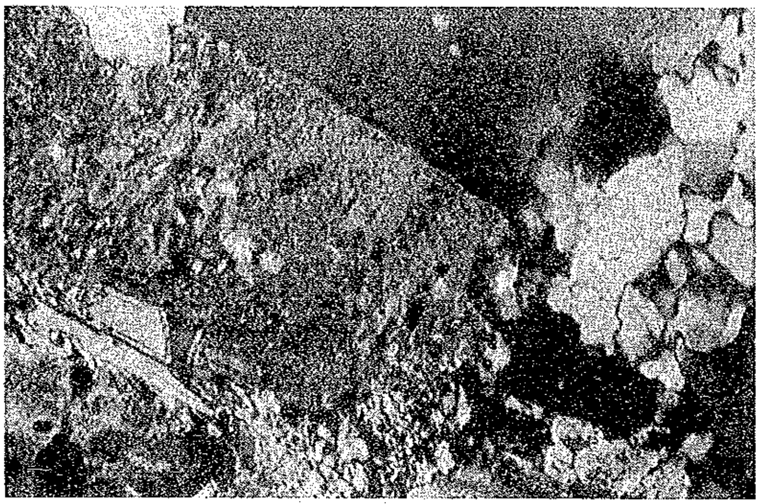

Crossed polars

0 0.5mm

Sample No. : FR–39
Location : Camarong River
Rock name : gneiss
Group name : Halcon metamorphics

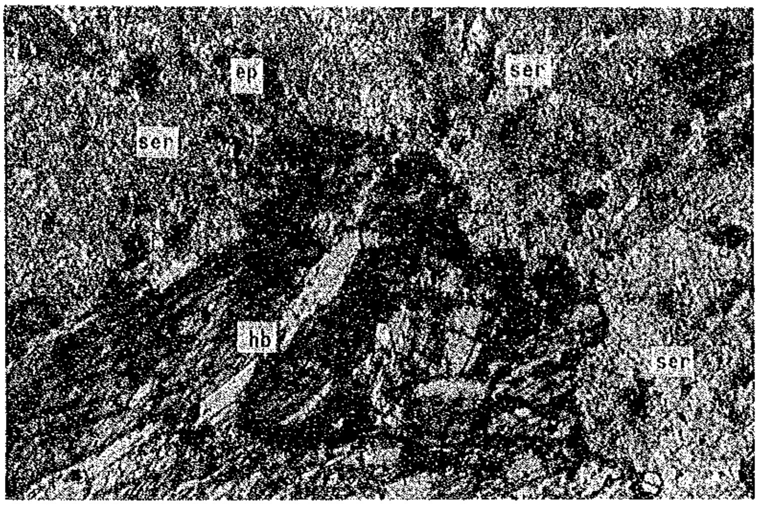

Only lower polar

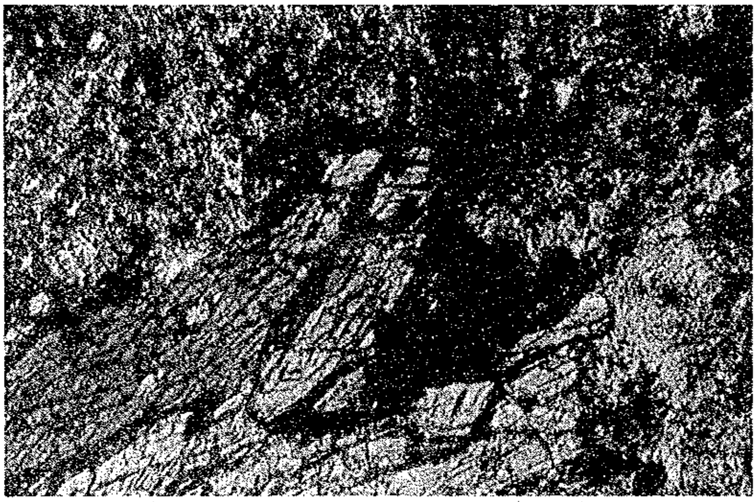

Crossed polars

0 0.5mm

Sample No.	:	FR–118
Location	:	east of Abra de Ilog
Rock name	:	metagabbro
Group name	:	Halcon metamorphics

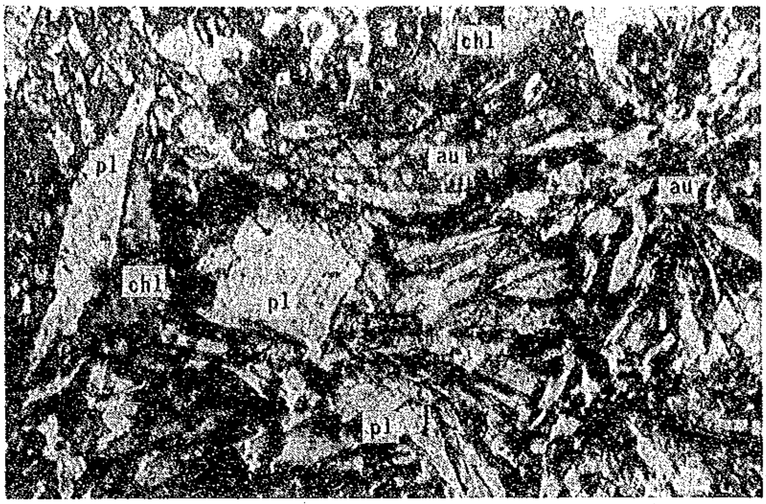

Only lower polar

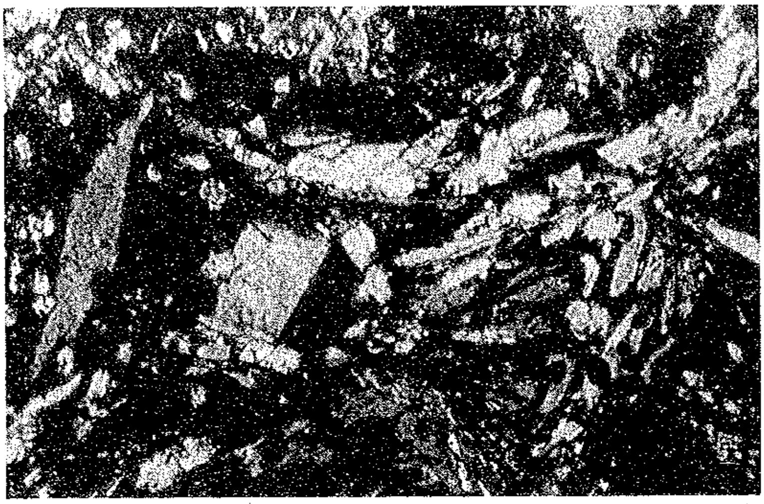

Crossed polars

0 0.5mm

Sample No. : YR–26
Location : Pola River
Rock name : basalt
Formation name : Lumintao formation

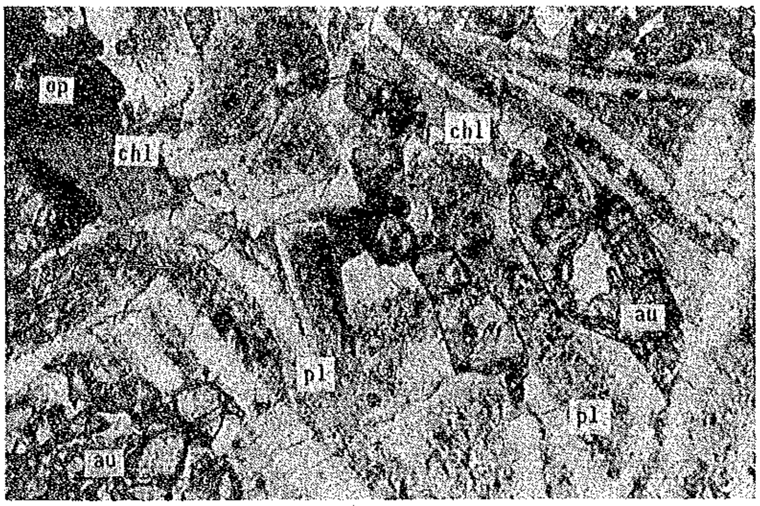

Only lower polar

Crossed polars

0 0.5mm

Sample No.	:	YR–10
Location	:	Rayusan River
Rock name	:	dolerite
Formation name	:	Lumintao formation

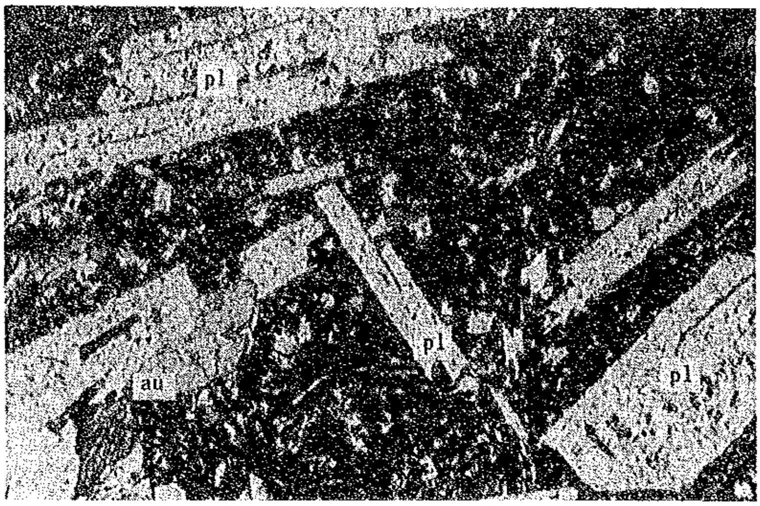

Only lower polar

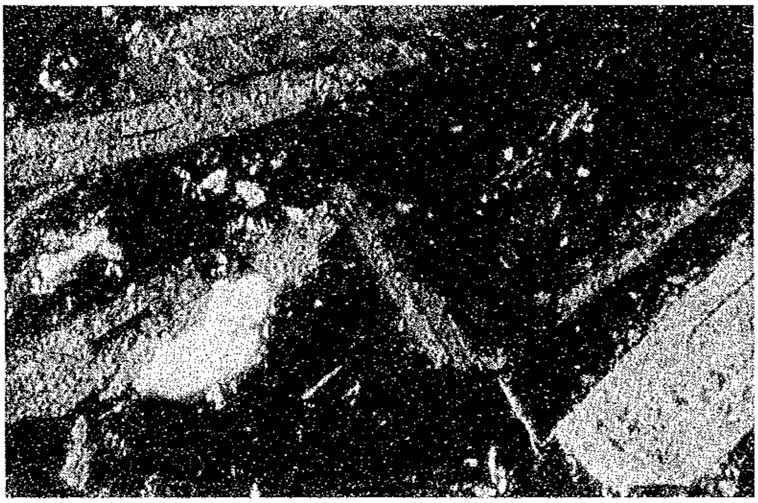

Crossed polars

0 0.5mm

Sample No.	:	FR–17
Location	:	Mamburao River
Rock name	:	basalt
Group name	:	Mamburao group

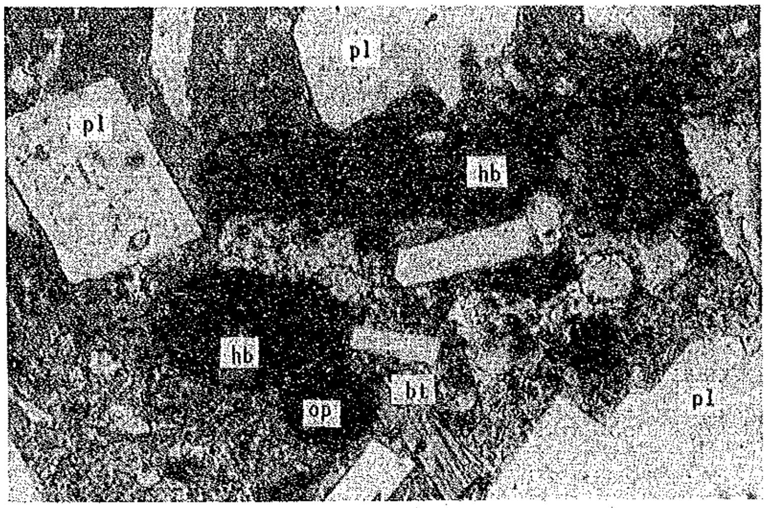

Only lower polar

Crossed polars

0 0.5mm

Sample No. : SR–93
Location : north of Calapan
Rock name : biotite hornblende andesite
Group name : Socorro group

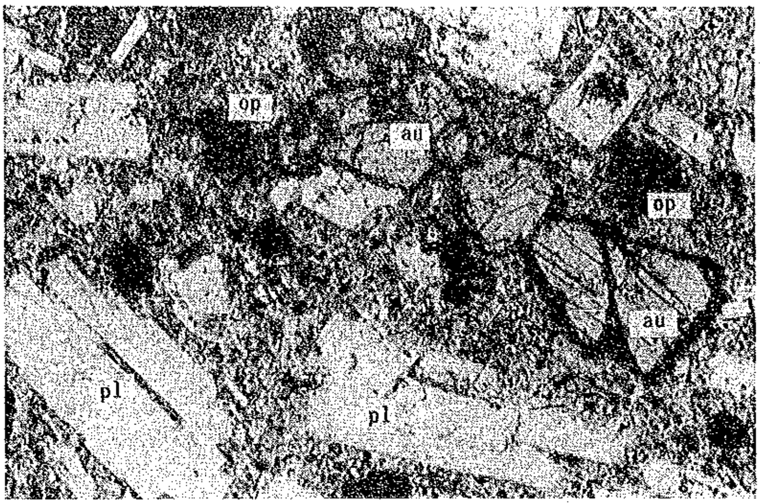

Only lower polar

Crossed polars

0 0.5mm

Sample No.	:	SR–72
Location	:	south of Mt. Dumali
Rock name	:	pyroxene andesite
Group name	:	Socorro group

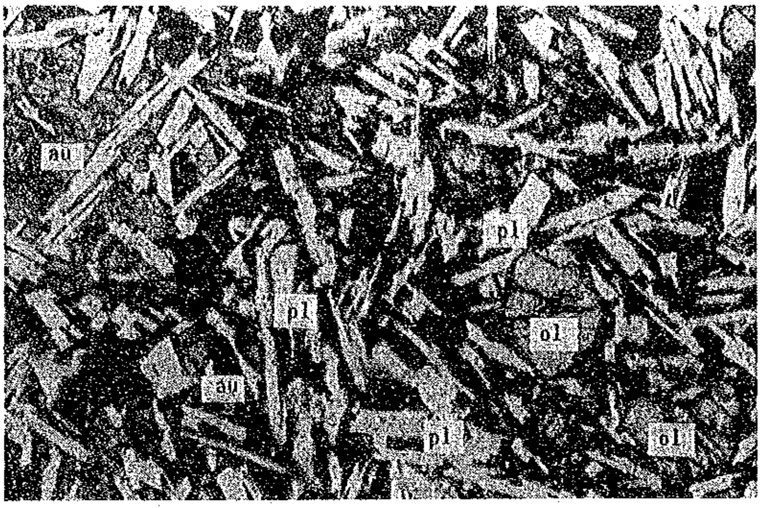

Only lower polar

Crossed polars

0 0.5mm

Sample No. : WR–32
Location : Mauhao
Rock name : basalt
Group name : Socorro group

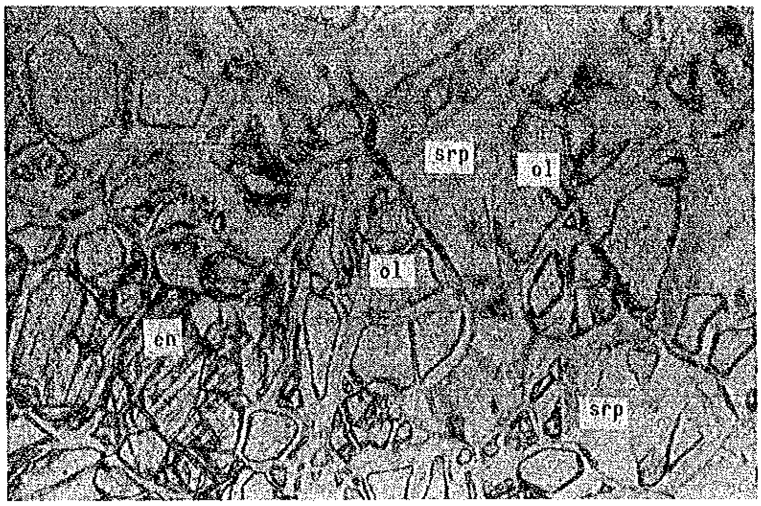

Only lower polar

Crossed polars

0 0.5mm

Sample No. : SR–65
Location : Bansud River
Rock name : harzbergite

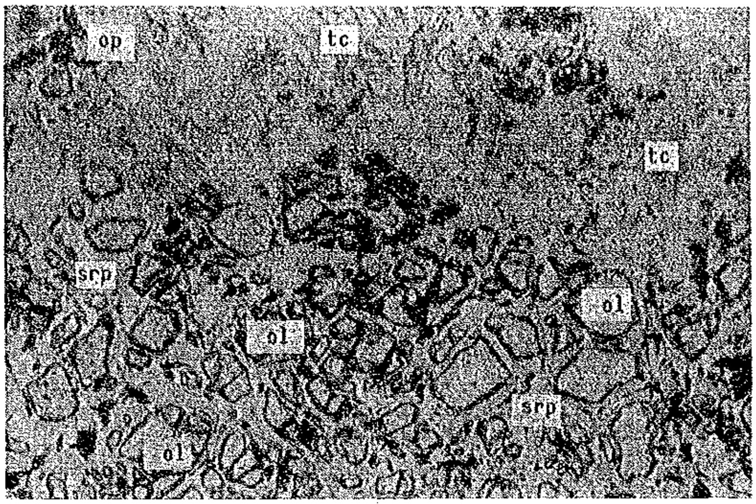

Only lower polar

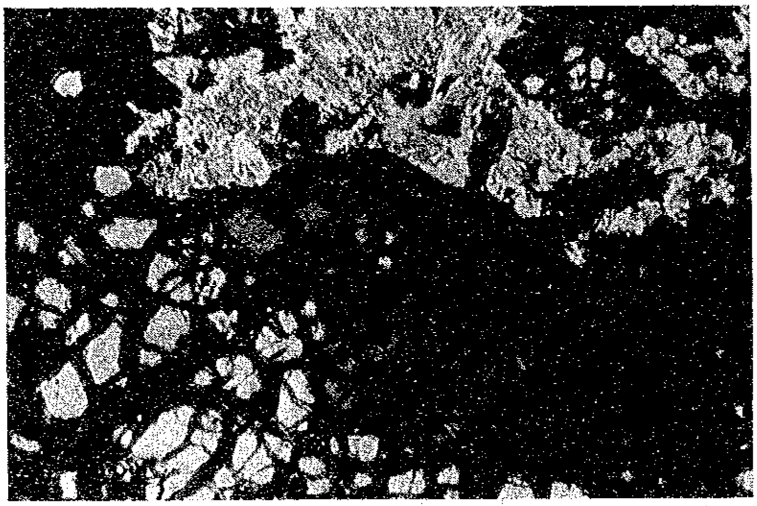

Crossed polars

0 0.5mm

Sample No. : WR–161
Location : Magaswangtubig River
Rock name : lherzolite

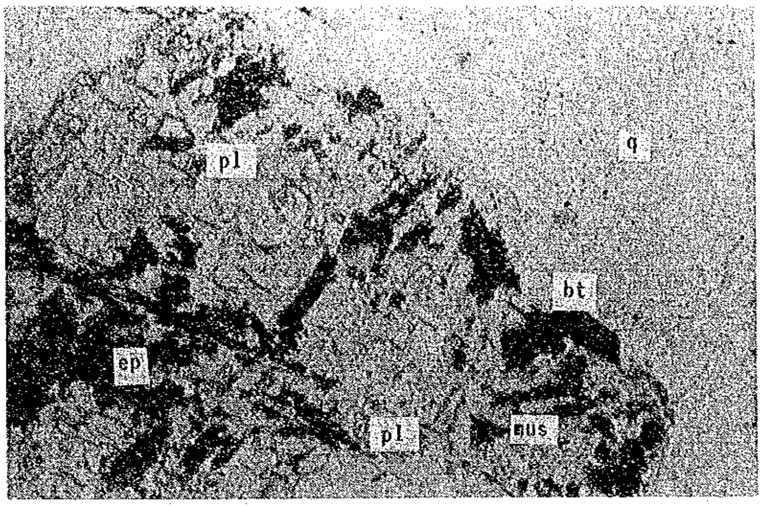

Only lower polar

Crossed polars

0 0.5mm

Sample No. : FR–41
Location : Camarong River
Rock name : granodiorite

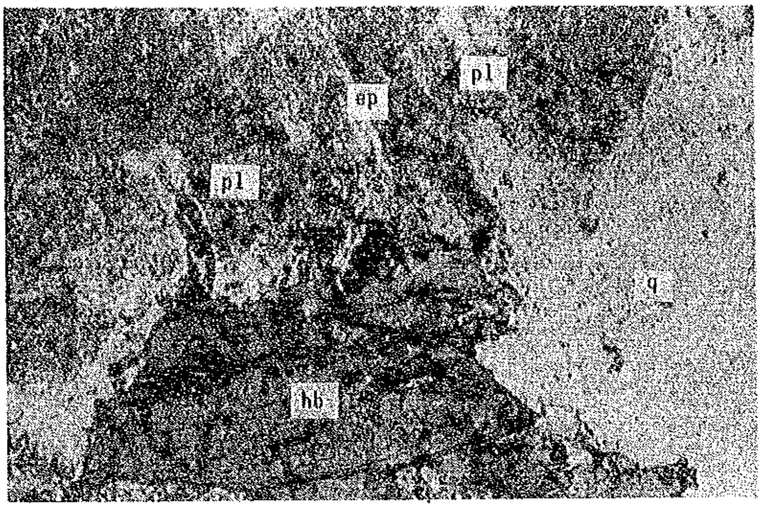

Only lower polar

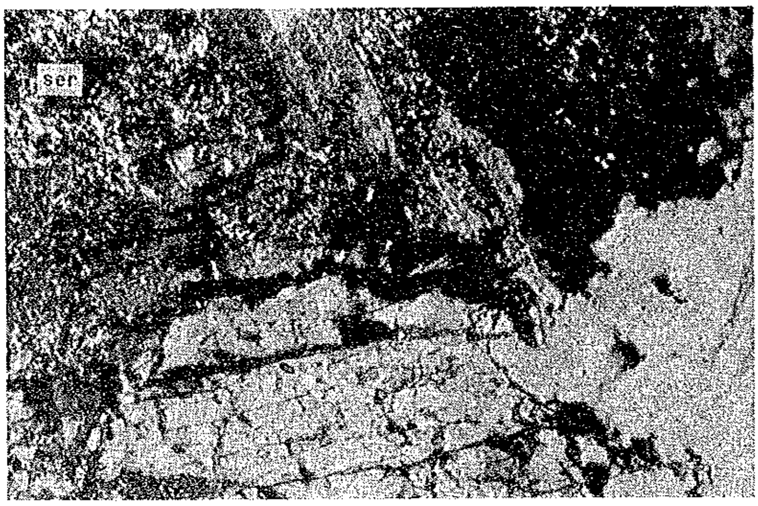

Crossed polars

0 0.5mm

Sample No. : FR–24
Location : Mamburao River
Rock name : quartz diorite

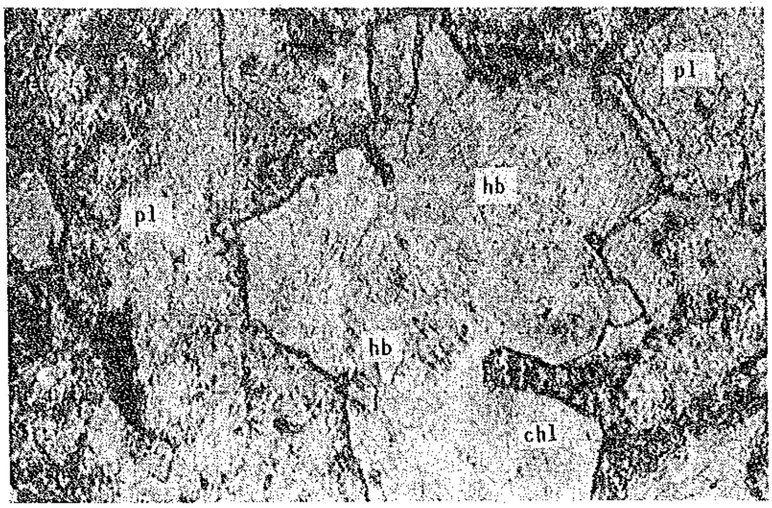

Only lower polar

Crossed polars

0 0.5mm

Sample No. : WR–179
Location : Magaswangtubig River
Rock name : diorite

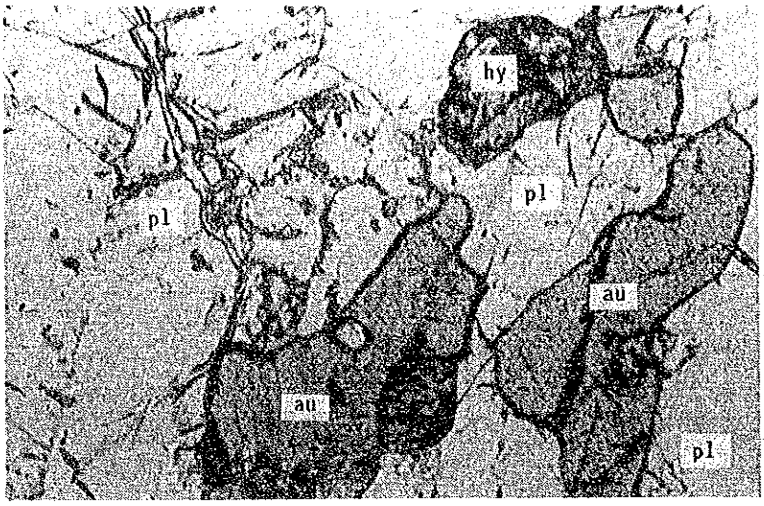

Only lower polar

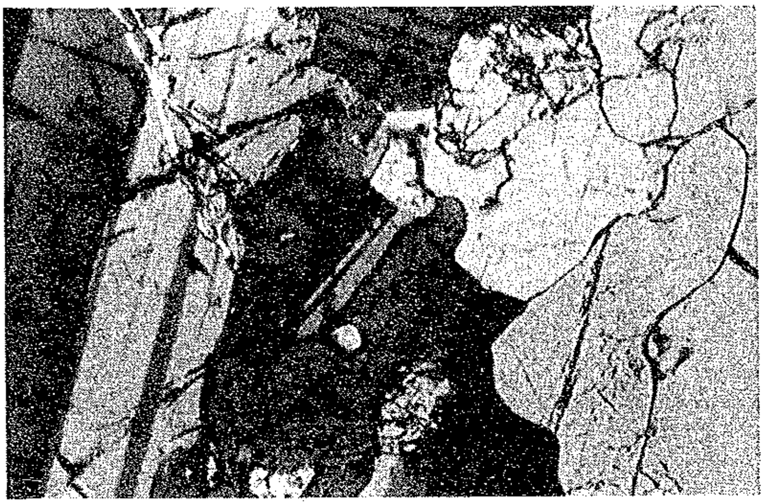

Crossed polars

0 0.5mm

Sample No. : YR–05
Location : Amnay River
Rock name : gabbro

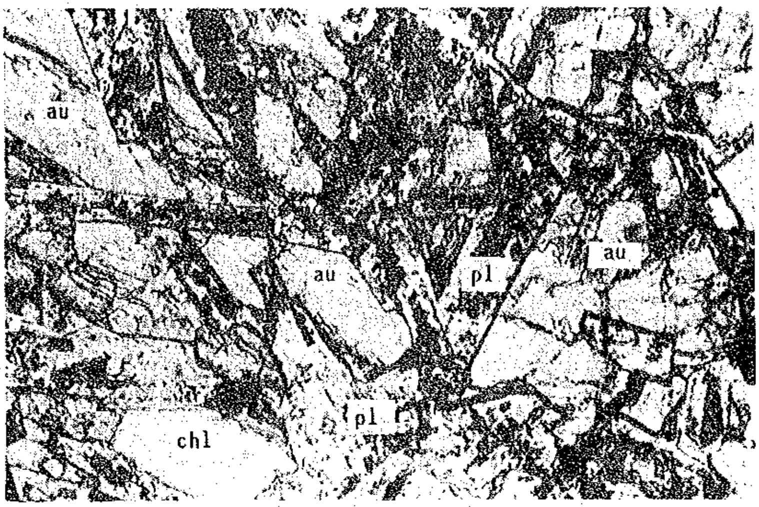

Only lower polar

Crossed polars

0 0.5mm

Sample No. : YR–20
Location : Rayusan River
Rock name : dolerite

Fig. A-2 Microphotograph of Polished Section

Abbreviation

cr	:	cromite
mg	:	magnetite
he	:	hematite
pyr	:	pyrrhotite
cp	:	chalcopyrite
sph	:	sphalerite

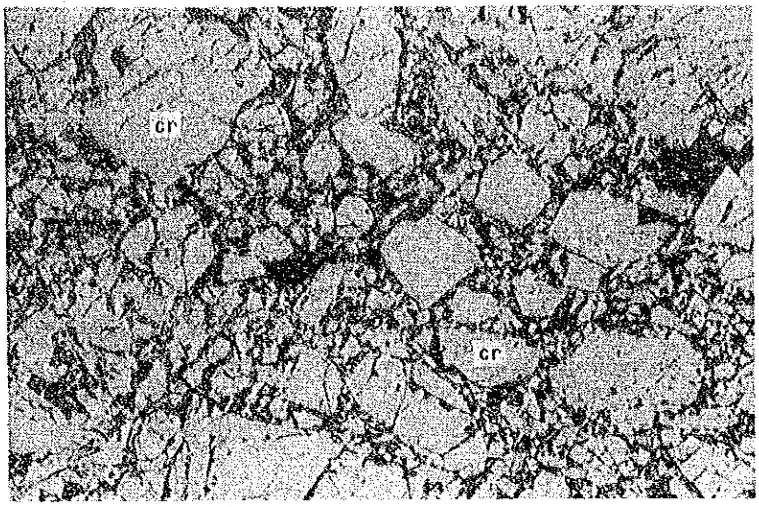

0 0.5mm

Sample No. : FR–07
Location : Paluan
Ore name : chromite ore

Refrected light
Only lower polar

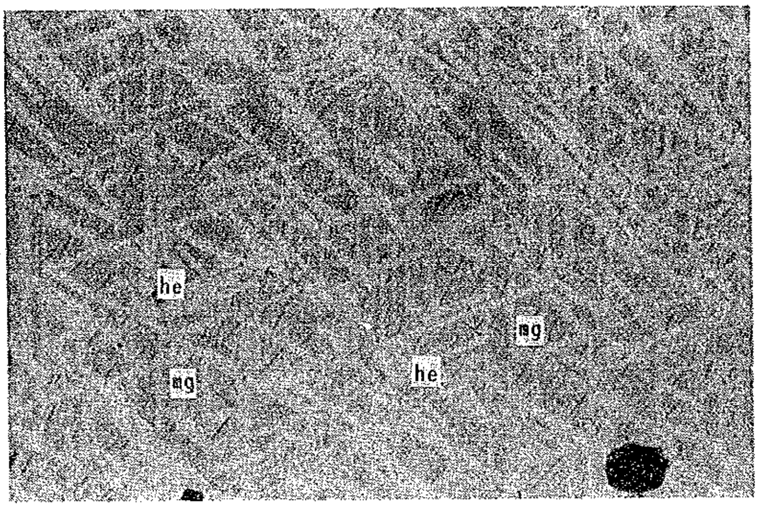

0 0.5mm

Sample No. : FR–45
Location : Pagbahan River
Ore name : magnetite ore

Refrected light
Only lower polar